

Gettering of iron by oxygen precipitates

H. Hieslmair,^{a)} A. A. Istratov,^{b)} S. A. McHugo,^{c)} C. Flink, T. Heiser,^{d)} and E. R. Weber
Department of Materials Science and Mineral Engineering, University of California at Berkeley, Berkeley, California 94720-1760

(Received 2 December 1997; accepted for publication 21 January 1998)

In order to better understand and model internal gettering of iron in silicon, a quantitative investigation of iron precipitation in silicon containing different oxygen precipitate densities was performed. The number of iron precipitation sites was obtained from the iron precipitation kinetics using Ham's Law. At low temperatures, the iron precipitate density corresponded to the oxygen precipitate density. A strong temperature dependence of the iron precipitate density was observed for the samples with larger oxygen precipitate densities. These data were used to simulate iron precipitation during a slow cool. From those simulations, optimal cooling rates were obtained for different silicon materials assuming various iron precipitation site densities in the epitaxial layer.
 © 1998 American Institute of Physics. [S0003-6951(98)00112-0]

For years, the integrated circuit (IC) industry has exploited the internal gettering effects of oxygen precipitates in the bulk silicon wafer to improve device yields. The oxygen precipitates and/or associated structural defects serve as heterogeneous precipitation sites for any supersaturated, mobile impurities, such as copper, nickel, iron, and cobalt. The gettering process occurs during a slow cool from high temperatures. Any mobile and supersaturated impurities can quickly precipitate only in regions of the silicon wafer which contain high concentrations of precipitation sites. In these regions, the dissolved impurity concentration never deviates significantly from the equilibrium solubility. In neighboring regions of low nucleation site densities, supersaturated impurities cannot precipitate quickly, and thus may significantly exceed the equilibrium solubility. This difference in precipitate site density creates an impurity concentration gradient during a slow cool. Supersaturated impurities diffuse away from the surface/device region, into the bulk where high concentrations of oxygen precipitates have been formed. This process is often referred to as relaxation gettering since it requires a supersaturation of impurities to "relax" to equilibrium concentrations during a cooling step.

Though there have been various studies on gettering by oxygen precipitates, few have been attempted to quantify gettering efficiency. Gilles *et al.*^{1,2} measured the low temperature precipitation rate of iron and derived nr_0 products, where n is the density of precipitation sites with a radius of r_0 . They showed a direct correlation between the nr_0 product of oxygen precipitates during the oxygen precipitate growth step and the nr_0 product of iron in the same samples at low temperatures. This established a link between iron precipitation and the presence of oxygen precipitates, al-

though the exact nature of the oxygen precipitate-related gettering was not established. Gilles *et al.* also suggested that the nr_0 product could be used in the future to quantify gettering efficiency.

As impurity concentration limits become more stringent, gettering processes need to be optimized. Computer simulations are the only viable method to predict and optimize the complicated processes of diffusion and precipitation during various temperature cycles. However, material properties first need to be quantified by meaningful parameters before computer simulations can be used. An obvious measure of efficiency of any relaxation gettering technique is the effective number and the location of impurity heterogeneous nucleation sites formed.

This study attempts to determine how iron is gettering by oxygen precipitates, to find a quantitative metric which describes the iron precipitation, and then to use experimental data in a simulator to obtain optimal cooling rates for relaxation gettering.

Czochralski silicon samples used in our experiment were cleaved from the center regions of four different wafers, all with an initial oxygen level of approximately $7 \times 10^{17} [\text{O}_i]/\text{cm}^3$ and a boron doping of $1.5 \times 10^{15} \text{ B}/\text{cm}^3$. These wafers were first heat treated to dissolve all oxygen nuclei, and then subjected to different oxygen nucleation treatments and finally a single 1000 °C, 16 h growth step. The resulting drop in oxygen concentration and the oxygen precipitate density are listed in Table I. Oxygen precipitate concentrations were obtained near the center of the cleaved wafers by preferential etching and then counting the pits. Samples for this experiment were taken near the center of unetched wafers. These samples were cleaned, scratched with 99.997% pure iron, and annealed at ≈ 900 °C, contaminating the samples to $(2-4) \times 10^{13} \text{ Fe}/\text{cm}^3$. The samples were cleaned again and annealed (precipitation anneal) in a horizontal furnace or in a rapid thermal anneal system followed by a rapid quench to room temperature. After the precipitation anneal, more than 60 μm were etched from the surfaces and aluminum diodes were evaporated for deep level transient spectroscopy (DLTS) measurements.

^{a)}Electronic mail: hhiesl@argon.eecs.berkeley.edu or weber@socrates.berkeley.edu

^{b)}On leave of absence from the Institute of Physics of St. Petersburg State University, Ul'ianovskaya 1, Petrodvorets, St. Petersburg, 198904 Russia.

^{c)}Lawrence Berkeley National Laboratories, MS 2-400, Berkeley, CA 94720.

^{d)}On leave of absence from the University Louis Pasteur, Laboratoire PHASE/CNRS, BP20, F67037 Strasbourg Cedex, France.

TABLE I. Experimental data and calculated radius for various silicon samples used in this study.

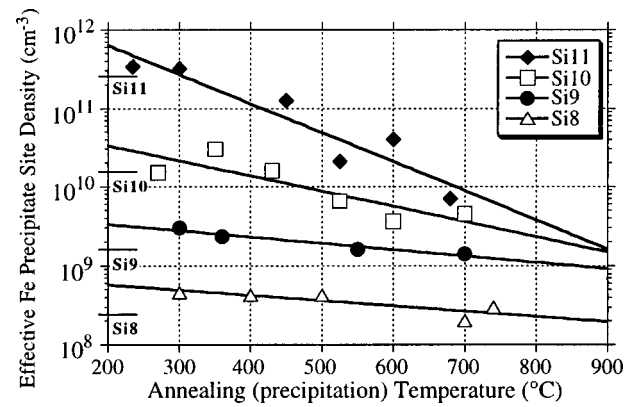
| Sample | ΔO_i ($\times 10^{17}$ O/cm ³) | n_{oxy} (Precip/cm ³) | Radius ($\times 10^{-6}$ cm) |
|--------|--|---|----------------------------------|
| Si8 | 0.28 | 2.3×10^8 | 8.38 |
| Si9 | 0.54 | 1.6×10^9 | 5.46 |
| Si10 | 2.25 | 1.5×10^{10} | 4.15 |
| Si11 | 6.00 | 2.5×10^{11} | 2.25 |

Ham's³ equations were used to determine the iron precipitation site concentration (see Ref. 4). Ham's equations relate the decay of a supersaturated impurity to the precipitate site density and the radius of the precipitate. Thus, $C = C(t, n, r_0, D)$ where C is the concentration of the dissolved impurity, n is the impurity site density, r_0 is the initial precipitate radius, and D is the impurity diffusivity. If the radius of the precipitate does not change, then the decay of the impurity concentration is a simple exponential decay with a time constant of $4\pi D n r_0$. However, if the precipitate is growing, then the decay is nonexponential which can still be simulated by iterative techniques.

Ham's equation was fitted to the experimental data points. The decay of interstitial iron from experiment was exponential, indicating that the radius was large and not growing. Such an exponential decay could be explained if iron were precipitating on or decorating a larger defect such as the oxygen precipitate itself. In this case, if the radius of the oxygen precipitate were used for r_0 , then the iron precipitate site⁵ density, n_{Fe} , should match that of the oxygen precipitate density, n_{Oxy} . Assuming the oxygen precipitates are essentially spherical, the radius of the oxygen precipitates was estimated from the number of precipitates and the total oxygen concentration precipitated. Using this calculated radius of the oxygen precipitates for r_0 , the resulting iron precipitate densities, n_{Fe} , for various annealing (precipitation) temperatures are shown in Fig. 1. One can see that for low temperatures, $n_{\text{Fe}} \approx n_{\text{Oxy}}$, proving the model that iron precipitates on or decorates the surface of the oxygen precipitates.

Additionally, for the Si8 and Si9, the low temperature n_{Fe} is even slightly above the n_{Oxy} as might be expected for an oxygen precipitate with a shape that has a larger surface area than a simple sphere. From Fujimori's⁶ study of oxygen precipitate morphology, we can expect that the oxygen precipitates in the Si11 sample have octahedral and truncated octahedral morphologies (essentially spherical), while the oxygen precipitates in the Si8 sample have truncated octahedral and platelet morphologies. The platelet morphology provides a larger surface area for the iron to precipitate on or decorate, resulting in a slightly larger n_{Fe} than n_{Oxy} .

In Fig. 1, one can also see that the low temperature data cannot be used at high temperatures, since there is a dependence of the iron precipitation site density on the annealing temperature. Therefore a better quantitative method for describing precipitation is to specify r_0 , thus determining the form of the decay, and then to specify n for various temperatures. The simplest explanation for the temperature dependence of n_{Fe} , is that at lower supersaturation (high temperature), not all of the oxygen precipitates act as sinks for iron.

FIG. 1. Effective iron precipitate density plotted for various temperatures using the radius of the oxygen precipitates for r_0 . The horizontal bars on the y axis indicate the oxygen precipitate density for the materials specified.

This implies that some of the oxygen precipitates are more favorable sites for iron precipitation. That the temperature effect is strongest for the Si11 samples which contain the smallest oxygen precipitates may indicate that there is a size or a strain⁷ effect. It seems more likely, however, that some sites on the oxygen precipitate itself are more favorable for iron precipitation. Thus at low supersaturation (high temperatures) only a portion of the oxygen precipitate surface serves as an iron precipitation site, reducing the effective number of sites. At high supersaturation (low temperatures), the whole oxygen precipitate behaves as a precipitate site, increasing the effective n_{Fe} .

By using straight line approximations to the observed temperature dependence of n_{Fe} (Fig. 1) in a simulator, one can simulate the precipitation of iron during a slow cool. The results of such simulations are shown in Fig. 2, which plots the remaining dissolved iron concentration as a function of time as a wafer cools from 850 °C at 80 °C/min, such that after 480 s, the wafer temperature is 200 °C. The equilibrium solubility⁸ is also plotted as a function of cooling time (the bottommost curve in Fig. 2).

Two curves are shown for the Si11 material; one with a constant value for n_{Fe} equal to the low temperature density only, and the other with a temperature dependent n_{Fe} . The difference between the two curves clearly shows that ignoring the temperature dependence of the iron precipitate site density, n_{Fe} , can lead to large errors in the dissolved iron concentration. Additionally, one can see that for large values of n_{Fe} the dissolved iron concentration never deviates significantly from the equilibrium solubility concentration (for example, the curve "Si11 $n = \text{constant}$ " in Fig. 2). As n_{Fe} becomes smaller, the rate of iron precipitation slows, and more of the iron is left dissolved after the slow cool.

A figure of merit (FOM) for the gettering process can be determined. We wish to maximize the product of flux and time of the impurities diffusing out of the device region, i.e., a denuded zone or epitaxial layer, and into the bulk. Flux is simply expressed as $J = -D \cdot \Delta C / \Delta x$. Δx is the distance between the device region and the bulk material, and ΔC is the difference in concentration between the device region and the bulk. Clearly, the flux increases with decreasing Δx , which should always be minimized. In this figure of merit, a worst case Δx , i.e., thick layer, is assumed. Thus we wish to

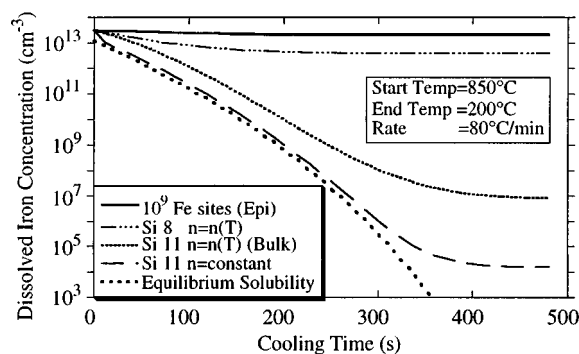


FIG. 2. Simulations of dissolved iron concentrations in various silicon materials during a slow cool of 80 °C/min, using the data from Fig. 1. The bottom curve is the equilibrium solubility during the slow cool. The difference between the two Si11 curves illustrates the error incurred by not taking into account the temperature dependence of n_{Fe} . The top two curves show how iron precipitates in a material with low oxygen precipitate concentrations and in an epitaxial layer, which is estimated to contain 1×10^9 iron nucleation ($r_0 \approx 2 \times 10^{-8}$ cm) sites/cm³.

maximize the product of D , ΔC , and t , the time of the process.

Consider a thick epitaxial layer with $n_{\text{Fe}} = 1 \times 10^9$ Fe nucleation sites/cm³ (top line in Fig. 2), and the bulk silicon with the same n_{Fe} as Si11 (curve labeled “Si11 $n=n(T)$ (Bulk)” in Fig. 2). Then the gettering driving force, ΔC , is the area between the lines labeled “Epi” and “Bulk” in Fig. 2. However, the area between the two curves must be weighted by the diffusivity of iron since the diffusivity is changing with temperature. Thus a (FOM) for the gettering efficiency for the slow cool described for Fig. 2 is

$$\text{FOM} = \int_0^{480 \text{ s}} D[T(t)] \cdot \Delta C(t) \cdot dt. \quad (1)$$

Figures of merit for various cooling rates and materials are shown in Fig. 3. The epitaxial layer was estimated to have either 1×10^9 or 1×10^8 iron nucleation sites/cm³. These estimates for n_{Fe} are based on precipitation studies performed on FZ and Cz silicon with no oxygen precipitates, which should in principle give an indication of the properties of an epitaxial layer.⁹ For a given epitaxial layer with 1×10^9 nucleation sites/cm³, one can see that the Si11 material with more oxygen precipitates has a better gettering efficiency at all cooling rates than the Si8 material which contains fewer oxygen precipitates. The optimal cooling rate, however, is the same. The other silicon materials, Si9 and Si10, performed similarly as the Si11 material because, at higher temperatures, the effective n_{Fe} for all three materials (Si9, Si10, and Si11) was $(1-8) \times 10^9$ oxygen sites/cm³. This illustrates that for large impurity concentrations, the gettering is strongly influenced by the high temperature characteristics of the materials. Improving the quality of the epitaxial layer by reducing the concentration of residual gettering sites can dramatically increase the gettering efficiency

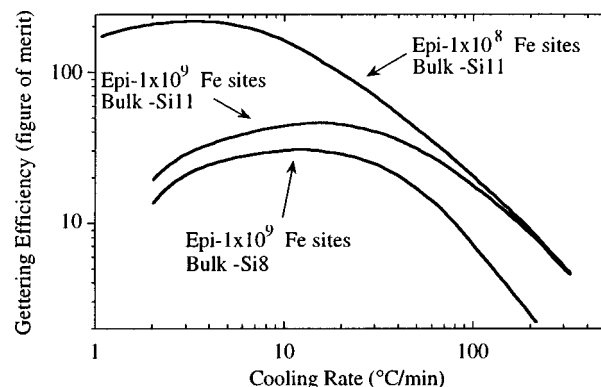


FIG. 3. Gettering efficiency vs cooling rate for different quality epitaxial layers and bulk materials.

provided that the cooling rate is slow enough. Such long processing times may not be practical. To save time, a slow cooling rate might be used until a medium temperature such as 520 °C is reached, followed by a fast cool. This should still provide efficient gettering since much of the gettering, at least down to 10^9 cm⁻³ (see Fig. 2) takes place above 520 °C.

In conclusion, iron precipitate densities, n_{Fe} , were measured for silicon with four oxygen precipitate densities. At low temperatures, the iron and oxygen precipitate site densities match, verifying that the whole oxygen precipitate surface acts as a sink for iron. The iron precipitate site density generally decreased with increasing temperature, with the strongest temperature dependence observed in samples with the highest oxygen precipitate concentration. The measured iron precipitate densities can be used in a simulator to obtain the decay of dissolved iron during a slow cool. These results can then be used to determine optimal cooling rates for various types of thick layers.

The authors would like to thank R. Falster and D. Gambino for supplying the Czochralski silicon. This work was partially funded by the WEDS consortium and the University of California MICRO program. The authors acknowledge the use of Lawrence Berkeley National Laboratories facilities which are funded through DOE.

¹D. Gilles, E. R. Weber, S. Hahn, O. R. Monteiro, and K. Cho, in *Semiconductor Silicon 1990*, edited by H. R. Huff, K. G. Barraclough, and J. Chikawa (Electrochemical Society, Pennington, NJ, 1990), p. 697.

²D. Gilles, E. R. Weber, and S. Hahn, *Phys. Rev. Lett.* **64**, 196 (1990).

³F. S. Ham, *J. Phys. Chem. Solids* **6**, 335 (1958).

⁴H. Hieslmair, A. A. Istratov, T. Heiser, and E. R. Weber (unpublished).

⁵The term “nucleation site” will be used for all sites with an initial radius of the smallest nucleus, i.e., a pair of atoms, which results in a nonexponential decay. The term “precipitation site” will refer to sites with a larger initial radius resulting in an exponential decay.

⁶H. Fujimori, *J. Electrochem. Soc.* **144**, 3180 (1997).

⁷S. A. McHugo, M. Mizuno, F. G. Kirscht, and E. R. Weber, *Appl. Phys. Lett.* **66**, 2840 (1995).

⁸E. R. Weber, *Appl. Phys. A: Solids Surf.* **30**, 1 (1983).

⁹H. Hieslmair (unpublished).